applied optics

Directional random laser source consisting of a HC-ARROW reservoir connected to channels for spectroscopic analysis in microfluidic devices

K. C. Jorge,[1] M. A. Alvarado,[2] E. G. Melo,[2] M. N. P. Carreño,[2] M. I. Alayo,[2] and N. U. Wetter[1,*]

[1]Centro de Lasers e Aplicações, Instituto de Pesquisas Energéticas e Nucleares, IPEN–CNEN/SP, São Paulo, Brazil
[2]Departamento de Engenharia de Sistemas Eletrônicos, Escola Politécnica, Universidade de São Paulo, São Paulo, Brazil
*Corresponding author: nuwetter@ipen.br

Received 18 March 2016; revised 17 May 2016; accepted 6 June 2016; posted 6 June 2016 (Doc. ID 261502); published 7 July 2016

Light sources are used in optofluidic devices for real-time system control and quantitative analysis of important process parameters. In this work, we present a random laser source using a hollow-core antiresonant reflecting optical waveguide (HC-ARROW) containing the gain media inside a reservoir to reduce dye bleaching, which is connected to microchannel waveguides to increase beam directionality. The device is pumped externally and emits a highly coherent and collimated laser beam.

OCIS codes: (140.3460) Lasers; (290.1990) Diffusion; (290.4210) Multiple scattering; (140.2050) Dye lasers.

http://dx.doi.org/10.1364/AO.55.005393

1. INTRODUCTION

Optofluidics is the combination of optics with microfluidics, which allows, in a single device, the integration of all functions necessary to create biosensors, molecular imaging tools, energy production, lab-on-chips, and much more. The key role of the optics part of optofluidics is to assess and quantify optical parameters of the chemical and physical reactions in these devices. These collected data in turn may be used to take control of flow rates, temperature, and other physical or chemical parameters of the lab-on-chips [1–3].

Traditional waveguide lasers generally require very high-end fabrication materials such as doped ultrapure glasses or silicon substrates and are also in need of expensive fabrication methods such as metalorganic chemical vapor deposition, femtosecond direct writing, and molecular beam epitaxy that are time-consuming methods which require several fabrication steps and optical polishing [4].

The idea to miniaturize a dye laser in order to gain a simpler and compact coherent light source has been shown before, where some researchers used mirrors for feedback [5,6] while others used distributed feedback [7,8]. Both categories have been fabricated in glass and in polydimethylsiloxane (PDMS). These microfluidic devices require external pumps in order to circulate the liquid and avoid dye bleaching although, in at least one case, a complex system of valves has been incorporated into the optofluidic chip for recirculation of the dye [9]. However, all of these devices are still relatively complex to scale down because they need precise fabrication methods for incorporation of mirrors and gratings for distributed feedback.

Different from traditional lasers, optical feedback in random lasers is given by multiple scattering inside the active region, using scattering centers such as rutile, resulting in omnidirectional emission with, consequently, very low spatial coherence [10–12]. Therefore, potential applications require optimization of its performance, especially with respect to optical efficiency and directionality or radiance. Nevertheless, such random laser light sources are ideal for disposable lab-on-chip devices which are currently developed in a worldwide effort to improve global health, as for example through early detection of infectious diseases or the development of point-of-care testing devices [4,13,14]. In this sense, the possibility of making a lab-on-chip with an onboard light source by simply "injecting" a random laser into a microchannel opens doors to new and inexpensive, close to single-step manufacturing methods, making the widespread use of such devices possible.

Light guiding of the emission of liquid random lasers inside special structures has been observed before and some examples are optical fibers and photonic-crystal fibers [15–17], dual-layered waveguide dye lasers [18], and liquid waveguide gain channels based on biological scatterers [19]. Such random lasers partly resolve the problem of beam directionality; however, the integration of these optofluidic lasers into a lab-on-chip device is only of limited practicability owing to their fabrication methods, materials, and, in some cases, complex structures [20–22].

The laser source reported here is composed of a reservoir containing the gain media (dye plus scattering centers), which is excited by an external pump laser, and the resulting laser beam is transported through a microchannel. Generally, light

propagation with low optical losses through low-index media such as gases and liquids is difficult. However, it has been demonstrated that antiresonant reflecting optical waveguides do resolve this problem [23,24]. In this work, a glass substrate containing a hollow-core antiresonant reflecting optical waveguide (HC-ARROW) reservoir and channel was used. No external pumps are required because the effect of dye bleaching is diminished by diffusion and convection inside the reservoir, which constantly replenishes the depleted dye inside the pump region [25]. The device is optimized with respect to laser efficiency and beam radiance. When pumped, the dye reservoir emits a highly coherent and collimated beam through the channel.

2. EXPERIMENTAL SETUP

The microfluidic device is composed of two Corning 7059 glass wafers on top of each other with dimensions of 10 mm × 20 mm × 0.9 mm [Fig. 1(a)]. A reservoir connected to two channels was etched into the lower glass wafer using conventional photolithography and humid etching for 10 min in a solution of 1:2:4 HF–HCl–DI with a rate of 4 μm/min, resulting in 40 μm channel depth and 260 μm channel width. The reservoir dimensions at its center were 3.6 mm × 10 mm × 0.04 mm ($W \times L \times D$). It is well established in microfluidic technology that this procedure produces surface roughness with R_a below 10 nm [26–28]. Furthermore, our channel dimensions are bigger than conventional waveguides and, therefore, losses are comparatively smaller [29]. Consequently, surface roughness in this case can be considered to not have a significant influence in light propagation [30]. It is also worth mentioning that simple characterization in an optical microscope showed no cracks in the waveguide, confirming good adhesion of the dielectric layers as expected.

A transfer matrix method was used to calculate the antiresonant multilayer parameters [31]. The etched side of the lower glass wafer and the bottom side of the cover glass wafer received seven alternate layers of TiO_2 (61 nm) and SiO_2 (300 nm) thin films, deposited by reactive magnetron sputtering using continuous O_2 flow, to achieve a maximum reflectance of 94% at the emission wavelength of our laser (550–630 nm), offering additional light confinement. For both TiO_2 and SiO_2 deposition, the Ar/N_2 flow ratio was 60/40 at 1 mTorr chamber pressure and 1.23 W/cm^2 power density. Figure 1(b) shows the calculated (dash) and the measured (solid) reflection spectra for the cover glass wafer using a normal incidence to the surface.

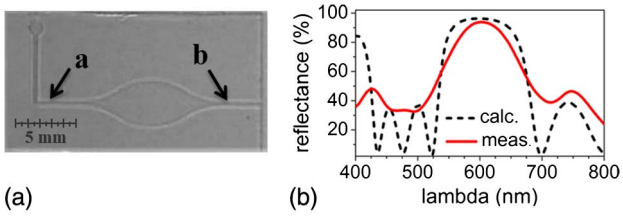

Fig. 1. (a) Picture of the bottom glass slide of the device showing the reservoir connected to two channels: *a* is the reservoir fill channel and *b* is the emission output channel. (b) Calculated (dashed line) and measured (solid line) reflectance spectra of the antiresonant coating.

The reservoir is transversely pumped at 532 nm by an optical parametric oscillator with a repetition rate of 10 Hz and a pulse duration of 9 ns. Using a cylindrical lens of 50 mm focal length, beam waist was formed in the form of a stripe with a width of 116 μm and length of 2.2 mm. This stripe of pump light was placed, by means of a steering mirror, along the long axis of the reservoir and aligned with the channels [Fig. 2(a)]. In this way, the directional laser emission, which is preferentially along the stripe direction, was effectively collected by channel *b* in Fig. 1 where it acted as waveguide. Alignment could be easily achieved as the focus stripe width was less than the channel width.

A dye solution of 2.1 mM Rhodamine 640 perclorate in ethylene glycol was chosen in order to achieve an absorption length longer than the depth of the device ($l_a = 220$ μm > 40 μm), guaranteeing good pump light absorption. The nonoptimal coating on the slides showed only 46% transmission at the pump wavelength, which caused losses for the incident pump beam but also allowed for some pump guidance inside the channel. A total of three internal reflections occurred before the pump power inside the channel decreased to $1/e^2$, allowing for good homogenization of the pump energy inside the channel.

The dye solution was divided into six samples containing TiO_2 nanoparticle scattering centers of 250 nm diameter in concentrations of (A) 0.14, (B) 0.29, (C) 0.58, (D) 1.00, (E) 2.40, and (F) 9.59 × 10^{10} cm^{-3}, respectively. From the size

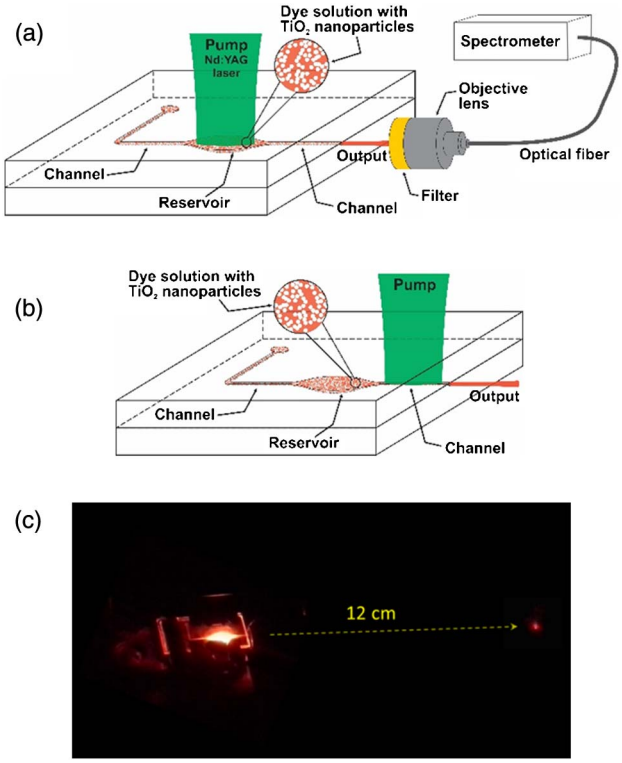

Fig. 2. (a) Pump setup used to generate laser action inside the reservoir. (b) Pump setup used to generate laser action inside the channel close to the laser's output port. (c) Picture of the red laser emission pointed at a sheet of paper located 12 cm away from the device's output.

and concentration data of the TiO_2 nanoparticles, the transport mean-free path, l_t, for each sample is estimated as in Ref. [31]. The value of l_t for sample A is 4.72 mm, B is 2.36 mm, C is 1.10 mm, D is 0.68 mm, and E is 0.34 mm. Therefore, these samples are considered to operate in the ballistic or weakly scattering regime, given that lt > la, meaning that within the active volume the photons have little chance of scattering, whereas outside the active volume they may become absorbed [32]. Only the transport mean-free path of sample F is smaller than the absorption length, namely, 0.09 mm. Thus, this sample can be considered as operating in the strongly scattering regime.

An additional pump setup, with the pump beam incident into the exit channel b instead of into the reservoir, was used for comparison, as shown in Fig. 2(b). Given the fact that in this setup the pump inversion is created closer to the output of the laser emission, one would expect a higher yield in this configuration when compared to the pump setup of Fig. 2(a), the reason being that less reabsorption occurs and that less scattering centers are in between the pump region and the laser's output port. These scattering centers that are not involved in the laser generation mechanism represent a passive loss.

Measurements were performed as a function of the pump pulse energy, which varied from 3.3 μJ to 0.63 mJ. The emission was filtered with a longpass filter (cut-on wavelength of 550 nm) and collected through an objective lens connected to an optical fiber that was coupled to a spectrometer of 0.06 nm spectral resolution. Figure 2(c) shows the device when operating and the directional laser emission. The picture was obtained with sample E when pumped with an energy of 100 μJ. It shows the highly directional and intense emission of the laser when pumped by the green laser.

3. RESULTS

Figure 3 shows the peak emission and the linewidth (FWHM) as a function of the pump pulse energy of the device filled with samples A to C and F. The measurements represented by square symbols were obtained for pumping into the reservoir (RES), and circles represent the results of pumping into the channel (CH). The results of samples D and E are not shown in Fig. 3 because they showed only intermediate results when compared to samples C and F.

In the graphs on the left-hand side of Fig. 3, we see the typical input–output curve of laser-like emission as a function of pump energy (in logarithmic scale), showing a clear threshold, especially for the first setup (reservoir). The reservoir shows clearly higher slope efficiency in most cases, except for sample F at high pump powers (>0.4 mJ), which is due to increased passive losses in the channel given the high scatterer density of this sample.

The graphs on the right-hand side of Fig. 3 show line width narrowing for both configurations. At very low scattering center density, there is no clear threshold when pumping into the channel [samples A and B; Figs. 3(a)–3(d)], showing the predominance of spontaneous emission and only little contribution of coherent emission [33]. At higher scattering center density (samples C and F), both configurations follow the same line narrowing behavior as expected.

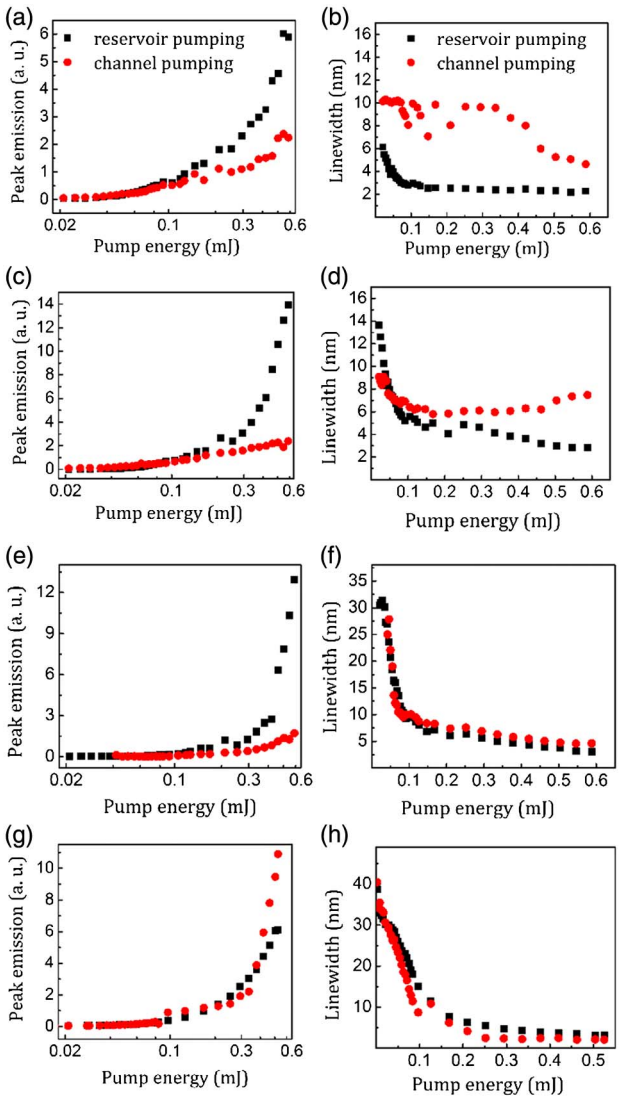

Fig. 3. Peak emission as functions of the pump pulse energy for (a) sample A, (c) sample B, (e) sample C, and (g) sample F when pumping into the reservoir (squares) and into the channel (circles). Graphs (b), (d), (f), and (h) show the respective emission linewidth (FWHM) narrowing as a function of pump pulse energy.

The laser threshold of the reservoir decreases from 1.2 mJ/mm^2 for sample B in Fig. 3(c) to 0.4 mJ/mm^2 for sample F in Fig. 3(g). It is important to note that this laser threshold is similar to values found in the literature for traditional (not random) optofluidics lasers [34]. An output energy of 1.2 μJ was measured for group E at 2 mJ of pump energy with a corresponding slope efficiency of 0.07%. For comparison, the highest slope efficiency reported in the literature, to the best of our knowledge, is 0.7% using neodymium-doped powders [35].

In Fig. 4(a), we show the normalized spectra of sample C under maximum pump pulse energy (0.6 mJ) for both setups. Even at maximum pump energy, the RES setup (solid line) shows a much cleaner emission spectrum. Not only is the emission spectrally narrower (3 nm as opposed to 4.5 nm in the CH setup), but the reabsorption in the channel also clears

the lower wavelength tail, resulting in a symmetric emission spectrum.

This is also shown in Fig. 4(b), which shows the peak value of the emission and the spectrally integrated values of sample *A* as functions of the pump pulse energy for the RES setup. Even the integrated spectrum shows a clear threshold behavior, which is different from what is observed in bulk random lasers. The result is a consequence of the directional emission above threshold [15,36]. This behavior was observed for all concentrations of scattering centers, even at very low concentrations as with sample *A*.

In order to determine the precise amount of coherent emission in both setups, the β factor was determined, which indicates the fraction of spontaneous radiation that participates in the laser emission [37,38].

The β factor was calculated according to the procedure described in [38] and corresponds to an average value of all samples for each setup. For the RES setup, β was 0.064 ± 0.011, indicating that only 6.4% of spontaneous emission participated in the total emission. For the CH setup, β was 0.126 ± 0.090, indicating that 12.6% of spontaneous emission contributed to the total emission. Therefore, the average β factor of the CH setup is twice that of the RES setup, demonstrating a lower quality emission. For comparison, the β value of the RES setup (0.064) is lower than for random lasers generated in bulks, in which β is equal to 0.10, and higher than in random fiber lasers where β is equal to 0.014 and which are considered highly coherent even when compared with some conventional lasers [15].

The RES setup not only shows consistent performance, maintaining stable behavior of the random laser even when varying the concentration of the scattering centers or the pump pulse energy, but it also ultimately emits a highly collimated coherent beam at the device's output port [15,39].

Figure 5 shows the output beam impinging on white paper after passing through a longpass filter (cut-on wavelength of 550 nm) when pumping sample *D* into the reservoir with 0.42 mJ of pulse energy. The divergence angle of the random laser emission was measured at 0.42 mJ of pump pulse energy for sample *D*. The full divergence angle (FWHM) of the RES setup was 68 mrad, while for the CH setup it was 129 mrad. For comparison, 68 mrad is the divergence of a Nd:YAG laser beam with a M^2 value of 10 (given the channel width of

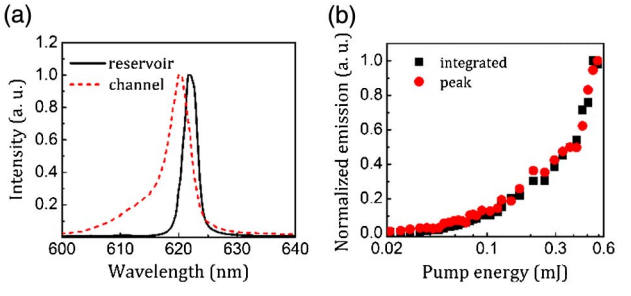

Fig. 4. (a) Normalized intensity profile of the spectra of RES (solid line) and CH (dotted line) setups filled with sample *C* for 0.6 mJ of pump energy. (b) Normalized peak emission (squares) and the spectral power (circles) of the RES setup filled with sample *A* as functions of the pump pulse energy.

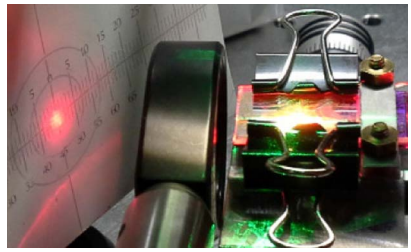

Fig. 5. Pictures of the red laser emission pointed at a sheet located 20 mm away from the longpass filter (black round object between the device and the sheet).

260 μm). This small divergence angle is a result of the ballistic photon propagation within the channel and the channel's dimensions. In the RES setup, photons enter the channel of 4 mm length and 260 μm width that serves as a geometrical aperture, resulting in a calculated divergence of 65 mrad. In a simplified model of the CH setup, photons are created in the middle of the channel and then pass on average through 2 mm of channel before they exit, resulting in a calculated divergence of 130 mrad. Both calculated values agree well with the measured divergences. In summary, the RES setup provides a highly directional beam that can be very useful for measuring strongly scattering and absorbing samples in microfluidics.

An additional experiment was performed to determine the temporal behavior of the deterioration of the rhodamine in both setups under continuous pumping. For this experiment, both devices were filled with sample *D* and pumped with a pulse energy of 0.6 mJ while their emission was recorded (Fig. 6). This sample was chosen because for both setups similar values of the output energy were obtained. The measured peak emission and peak wavelength are shown in Figs. 6(a) and 6(b), respectively. Comparison of the peak emissions shows that the temporal stability of the random laser signal during RES pumping is good, whereas a decay time of approximately 15 min occurs in the CH pump setup. The emission decreased 13% and 69.2% after 30 min, during RES and CH pumping, respectively. The photo degradation of the organic dye is prevented in the RES setup due its bigger volume that profits from better dye circulation, which reduces the exposure time of the dye molecules [30].

For comparison, a cuvette of 1 cm × 1 cm filled with a solution containing 10 times more TiO_2 particles and pumped with approximately twice our focus intensity showed a decay

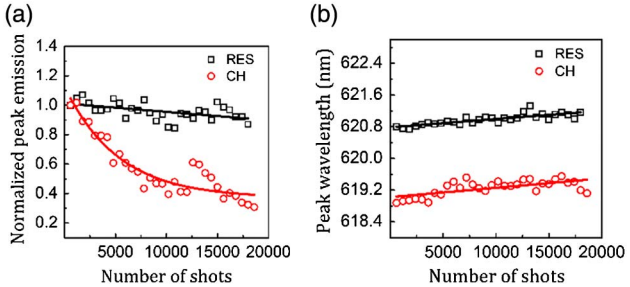

Fig. 6. (a) Normalized peak emission. (b) Peak wavelength as functions of the number of shots (20, 000 shots = 30 min) for RES and CH filled with sample *D* and pumped with an energy of 0.6 mJ.

of 84% after 2000 shots (~7 min) [40]. After the same time (equal to approximately 4200 shots in our case) the peak emission from our RES setup decreased by just 2%.

Variations of the peak emission wavelengths of both setups [Fig. 6(b)] are very small: $\lambda_0^{RES} = (621.0 \pm 0.1)$ nm and $\lambda_0^{CH} = (619.2 \pm 0.2)$ nm and are probably due to slight heating of the device which causes an increasing redshift. The RES setup showed a redshift of approximately 2 nm when compared to the CH setup because of reabsorption in the passive channel between the reservoir and the device's output port.

4. CONCLUSIONS

An optofluidic random laser source for lab-on-chip applications is presented. The HC-ARROW device is formed by a reservoir connected to two channels. Random laser performance was optimized as a function of scattering center density and compared for two setups: one with and the other without a reservoir. A lower laser threshold of below 100 μJ and a higher radiance was achieved in all cases when using the reservoir. Additionally, a much slower dye decay rate was observed when using the reservoir. In particular, the RES setup filled with sample C (0.58×10^{10} cm^{-3} scatterer density) presented the best performance when considering power efficiency. Another advantage of the reservoir is the narrow and symmetric emission spectra and the much higher degree of coherence given the small contribution of spontaneous emission.

The random laser source proposed here does not necessarily need to be fabricated by etching methods. For example, it could be injected or pressed into standard PDMS material and coated with silver paint for a second pass of the pump beam through the gain media. The highly directional laser beam and the absence of recirculating pumps make this device apt for typical lab-on-chip applications.

Funding. Coordenação de Aperfeiçoamento de Pessoal de Nível Superior (CAPES) (081/2013); Fundação de Amparo à Pesquisa do Estado de São Paulo (FAPESP) (2012/18162-4); Conselho Nacional de Desenvolvimento Científico e Tecnológico (CNPq) (2012_6/402241).

REFERENCES

1. G. M. Whitesides, "The origins and the future of microfluidics," Nature **442**, 368–373 (2006).
2. D. Psaltis, S. R. Quake, and C. Yang, "Developing optofluidic technology through the fusion of microfluidics and optics," Nature **442**, 381–386 (2006).
3. D. Erickson, D. Sinton, and D. Psaltis, "Optofluidics for energy applications," Nat. Photonics **5**, 583–590 (2011).
4. X. Fan and I. M. White, "Optofluidic microsystems for chemical and biological analysis," Nat. Photonics **5**, 591–597 (2011).
5. D. V. Vezenov, B. T. Mayers, R. S. Conroy, G. M. Whitesides, P. T. Snee, Y. Chan, D. G. Nocera, and M. G. Bawendi, "A low-threshold, high-efficiency microfluidic waveguide laser," J. Am. Chem. Soc. **127**, 8952–8953 (2005).
6. B. Helbo, A. Kristensen, and A. Menon, "A micro-cavity fluidic dye laser," J. Micromech. Microeng. **13**, 307–311 (2003).
7. W. Song, A. E. Vasdekis, Z. Li, and D. Psaltis, "Low-order distributed feedback optofluidic dye laser with reduced threshold," Appl. Phys. Lett. **94**, 051117 (2009).
8. W. Song, A. E. Vasdekis, Z. Li, and D. Psaltis, "Optofluidic evanescent dye laser based on a distributed feedback circular grating," Appl. Phys. Lett. **94**, 161110 (2009).
9. J. C. Galas, J. Torres, M. Belotti, Q. Kou, and Y. Chen, "Microfluidic tunable dye laser with integrated mixer and ring resonator," Appl. Phys. Lett. **86**, 264101 (2005).
10. R. V. Ambartsumyan, N. G. Basov, P. G. Kryukov, and V. S. Letokhov, "A laser with a nonresonant feedback," IEEE J. Quantum Electron. **2**, 442–446 (1966).
11. N. M. Lawandy, R. M. Balachandran, A. S. L. Gomes, and E. Sauvain, "Laser action in strongly scattering media," Nature **368**, 436–438 (1994).
12. H. Cao, Y. G. Zhao, S. T. Ho, E. W. Seelig, Q. H. Wang, and R. P. H. Chang, "Random laser action in semiconductor powder," Phys. Rev. Lett. **82**, 2278–2281 (1999).
13. E. K. Sackmann, A. L. Fulton, and D. J. Beebe, "The present and future role of microfluidics in biomedical research," Nature **507**, 181–189 (2014).
14. S. N. Bhatia and D. E. Ingber, "Microfluidic organs-on-chips," Nat. Biotechnol. **32**, 760–772 (2014).
15. C. J. S. de Matos, L. de S. Menezes, A. M. Brito-Silva, M. M. Gámez, A. S. L. Gomes, and C. B. de Araújo, "Random fiber laser," Phys. Rev. Lett. **99**, 153903 (2007).
16. R. M. Gerosa, A. Sudirman, L. de S. Menezes, W. Margulis, and C. J. de Matos, "All-fiber high repetition rate microfluidic dye laser," Optica **2**, 186–193 (2015).
17. Z. Hu, Q. Zhang, B. Miao, Q. Fu, G. Zou, Y. Chen, Y. Luo, D. Zhang, P. Wang, H. Ming, and Q. Zhang, "Coherent random fiber laser based on nanoparticles scattering in the extremely weakly scattering regime," Phys. Rev. Lett. **109**, 253901 (2012).
18. H. Watanabe, Y. Oki, M. Maeda, and T. Omatsu, "Waveguide dye laser including a SiO_2 nanoparticle-dispersed random scattering active layer," Appl. Phys. Lett. **86**, 151123 (2005).
19. H. Zhang, G. Feng, S. Wang, C. Yang, J. Yin, and S. Zhou, "Coherent random lasing from liquid waveguide gain channels with biological scatters," Appl. Phys. Lett. **105**, 253702 (2014).
20. B. N. S. Bhaktha, X. Noblin, and P. Sebbah, "Optofluidic random laser," Appl. Phys. Lett. **101**, 151101 (2012).
21. K. C. Vishnubhatla, J. Clark, G. Lanzani, R. Ramponi, R. Osellame, and T. Virgili, "Femtosecond laser fabrication of microfluidic channels for organic photonic devices," Appl. Opt. **48**, G114–G118 (2009).
22. N. Bachelard, S. Gigan, X. Noblin, and P. Sebbah, "Adaptive pumping for spectral control of random lasers," Nat. Phys. **10**, 426–431 (2014).
23. D. Yin, H. Schmidt, J. P. Barber, and A. R. Hawkins, "Integrated ARROW waveguides with hollow cores," Opt. Express **12**, 2710–2715 (2004).
24. D. Yin, H. Schmidt, J. P. Barber, E. J. Lunt, and A. R. Hawkins, "Optical characterization of arch-shaped ARROW waveguides with liquid cores," Opt. Express **13**, 10564–10570 (2005).
25. G.-H. Morten, S. Balslev, N. A. Mortensen, N. Asger, and A. Kristensen, "Bleaching and diffusion dynamics in optofluidic dye laser," Appl. Phys. Lett. **90**, 143501 (2007).
26. C. Iliescu, J. Jing, F. E. H. Tay, J. Miao, and T. Sund, "Characterization of masking layers for deep wet etching of glass in an improved HF/HCl solution," Surf. Coat. Technol. **198**, 314–318 (2005).
27. C. Iliescu, B. Chen, and J. Miao, "On the wet etching of Pyrex glass," Sens. Actuators A **143**, 154–161 (2008).
28. N. V. Toan, M. Toda, and T. Ono, "An investigation of processes for glass micromachining," Micromachines **7**, 51 (2016).
29. F. Ladouceur, J. D. Love, and T. J. Senden, "Effect of side wall roughness in buried channel waveguides," IEEE Proc. Optoelectron. **141**, 242–248 (1994).
30. T. Barwicz and H. A. Haus, "Three-dimensional analysis of scattering losses due to sidewall roughness in microphotonic waveguides," J. Lightwave Technol. **23**, 2719–2732 (2005).
31. D. O. Carvalho and M. I. Alayo, "a-SiC:H anti-resonant layer ARROW waveguides," J. Opt. A **10**, 104002 (2008).
32. J. Kitur, G. Zhu, M. Bahoura, and M. A. Noginov, "Dependence of the random laser behavior on the concentrations of dye and scatterers," J. Opt. **12**, 024009 (2010).

33. X. Wu, W. Fang, A. Yamilov, A. A. Chabanov, A. A. Asatryan, L. C. Botten, and H. Cao, "Random lasing in weakly scattering systems," Phys. Rev. A **74**, 053812 (2006).
34. S. K. Y. Tang, Z. Li, A. R. Abate, J. A. Agresti, D. Psaltis, D. A. Weitz, and G. M. Whitesides, "A multi-color fast-switching microfluidic droplet dye laser," Lab Chip **9**, 2767–2771 (2009).
35. M. A. Noginov, I. N. Fowlkes, and G. Zhu, "Fiber-coupled random laser," Appl. Phys. Lett. **86**, 161105 (2005).
36. M. P. van Exter, G. Nienhuis, and J. P. Woerdman, "Two simple expressions for the spontaneous emission factor β," Phys. Rev. A **54**, 3553–3558 (1996).
37. G. van Soest, F. J. Poelwijk, R. Sprik, and A. Lagendijk, "Dynamics of a random laser above threshold," Phys. Rev. Lett. **86**, 1522–1525 (2001).
38. G. van Soest and A. Lagendijk, "β factor in a random laser," Phys. Rev. E **65**, 047601 (2002).
39. H. K. Liang, S. F. Yu, and H. Y. Yang, "Directional and controllable edge-emitting ZnO ultraviolet random laser diodes," Appl. Phys. Lett. **96**, 101116 (2010).
40. A. M. Brito-Silva, A. Galembeck, A. S. Gomes, A. J. Jesus-Silva, and C. B. de Araújo, "Random laser action in dye solutions containing Stöber silica nanoparticles," J. Appl. Phys. **108**, 033508 (2010).